Int. J. Heat Mass Transfer. Vol. 28, No. 11, pp. 2149–2157, 1985
Printed in Great Britain

0017–9310/85 $3.00 + 0.00

Non-Darcian effects on vertical-plate natural convection in porous media with high porosities

J. T. HONG,* C. L. TIEN* and M. KAVIANY†
* University of California, Berkeley, CA 94720, U.S.A.
† University of Wisconsin, Milwaukee, WI 53201, U.S.A.

(*Received* 8 *February* 1985 *and in final form* 29 *May* 1985)

Abstract—The present analytical study on the non-Darcian effects on natural convection from a vertical plate embedded in a high-porosity medium shows that the boundary and inertia effects have a significant influence on the velocity profiles and surface heat transfer rate. Both effects are more pronounced in high-porosity media and reduce heat transfer from the heated plate. The boundary effect becomes more noticeable in the region close to the leading edge of the heated plate, while the inertia effect increases with downstream locations on a heated plate. The results also show that as the resistance due to the solid matrix increases, the velocity profile tends toward the conventional exponential form, which results from velocity slip at the boundary.

1. INTRODUCTION

TRANSPORT of momentum and thermal energy in fluid-saturated porous media with low porosities is commonly described by Darcy's model for conservation of momentum and by an energy equation based on the velocity field found from this model. In contrast to rocks, soil, sand and other media that do fall in this category, certain porous materials, such as foam metals and fibrous media, usually have high porosities. In these media, the boundary and inertia effects, not included in Darcy's model, may alter the flow and heat transfer characteristics. Therefore, it is necessary to determine the conditions under which these effects are important. For forced convection flows it has been shown that for Reynolds numbers based on particle or pore size larger than unity a velocity-square term must be added [1, 2]. Also, the viscous boundary layer develops very rapidly and then remains constant, and the Nusselt number decreases when the inertia and boundary effects become significant [3, 4].

A recent review of natural convection flow in porous media shows considerable research activity in this area [5]. The vertical flat plate natural convection flow was studied under boundary-layer and Darcy's approximations [6], and with the effects of axial conduction and the transverse pressure gradient [7]. The analysis for the inertia effect (accounted for by the velocity-square term) allows for velocity slip at the rigid boundary and shows that the Nusselt number decreases as the inertia effect becomes more pronounced [8, 9]. The boundary effect results in a smaller Nusselt number, but this difference decreases as the Rayleigh number increases [10]. Recent efforts have included the effects of the boundary term and the velocity-square term, as well as the nonhomogeneity in the porosity distribution near the wall in packed-sphere systems [11]. The results show that the wall-channeling effect, due to the high porosity near the wall, dominates and the non-Darcian effects are not significant in the regions away from the wall because of relatively low permeability considered.

The object of this work is to study the boundary and inertia effects on the transport of momentum and thermal energy for the natural convection boundary-layer flow near a vertical heated plate in high-porosity media. These non-Darcian effects, though not important in low-porosity media, are shown to be very significant in high-porosity media. Furthermore, for low-porosity media the entry region is usually very small, and the convective term in the governing equations can be neglected [3]. This may not be the case for high-porosity media. In this work, the developing effect (due to the convective term) is also included.

2. MATHEMATICAL FORMULATIONS

Consider a vertical heated plate with constant wall temperature T_w embedded in a porous medium. The temperature of the medium far away from the plate is T_∞. In order to study transport through high-porosity media, the original model of Darcy is improved by including boundary and inertia effects using volume-averaged principles and available empirical results [3]. In addition, the following assumptions are made for the formulation: the fluid and the porous medium are everywhere in local thermodynamic equilibrium; the porous medium is isotropic and homogeneous; properties of the fluid and the porous medium such as viscosity, thermal conductivity, thermal expansion coefficient and permeability are constant. Under these assumptions, the conservation equations become

$$\nabla \cdot \mathbf{u} = 0 \tag{1}$$

$$\frac{\rho_f}{\varepsilon^2}\mathbf{u}\cdot\nabla\mathbf{u} = -\nabla p + \rho_f g\mathbf{i} - \frac{\mu_f \mathbf{u}}{K} - \rho_f C|\mathbf{u}|\mathbf{u} + \frac{\mu_f}{\varepsilon}\nabla^2\mathbf{u} \tag{2}$$

$$\mathbf{u}\cdot\nabla T = \alpha_e \nabla^2 T \tag{3}$$

NOMENCLATURE

C inertia coefficient
Da_x local Darcy number, K/x^2
Da_L Darcy number, K/L^2
f dimensionless stream function
Gr_x local Grashof number, $g\beta_f\Delta T x^3/\nu_f^2$
Gr_L Grashof number, $g\beta_f\Delta T L^3/\nu_f^2$
$\widehat{Gr}$ Darcy-modified Grashof number, $g\beta_f\Delta T K^2 C/\nu_f^2$
g gravitational constant
K permeability
k_e effective conductivity
L characteristic length of the heated plate
Nu_x Nusselt number
Pr Prandtl number, ν_f/α_e
p pressure
q local heat flux
$\widehat{Ra}_x$ Darcy-modified Rayleigh number, $g\beta_f\Delta T K x/\nu_f\alpha_e$
T temperature
u velocity along the plate
v velocity perpendicular to the plate
x coordinate axis along the plate
y coordinate axis perpendicular to the plate.

Greek symbols
α_e effective thermal diffusivity
β_f coefficient of thermal expansion
Γ parameter, LC
δ_m hydrodynamic boundary-layer thickness
δ_t thermal boundary-layer thickness
ε porosity
ζ dimensionless coordinate along the plate, x/L
η dimensionless coordinate perpendicular to the plate, $(y/x)(Gr_x/4)^{1/4}$
θ dimensionless temperature
μ_f fluid dynamic viscosity
ν_f fluid kinematic viscosity, μ_f/ρ_f
ξ parameter, $2\zeta^{1/2}/Gr_L^{1/2}\,Da_L$
ρ_f fluid density
Φ parameter, $(2Gr_L^{1/2}Da_L)$
ψ stream function.

Superscript
′ derivative with respect to η.

Subscripts
∞ at a distance from the wall
w evaluated at wall
η derivative with respect to η
ξ derivative with respect to ξ
ζ derivative with respect to ζ.

where $\mathbf{i}$ is the unit vector opposite to gravity; $\mathbf{u}$ is the Darcian velocity; T, p and g are the temperature, pressure and gravitational constant; ρ_f, μ_f and β_f are the density, viscosity and thermal expansion coefficients of the fluid; $\alpha_e = k_e/(\rho_f c_f)$ is the effective thermal diffusivity of the medium with $\rho_f c_f$ denoting the product of density and specific heat of the fluid, and k_e is the effective thermal conductivity of the saturated porous medium. K and C are the permeability and the inertia coefficients of the porous medium and are dependent on the porosity ε and other geometrical parameters of the medium. When the porosity of the medium approaches unity (all the pores are assumed to be well connected) K approaches infinity and C approaches zero; therefore, equations (1)–(3) approach those for natural convection in a Newtonian fluid (i.e. no solid matrix is present). It is also noted that these equations do not include the 'dispersion effects' since the magnitudes of the dispersion diffusivities are not clearly known.

Consider a coordinate system with x along the vertical heated plate and y perpendicular to it. By introducing a stream function ψ and employing the boundary-layer and Boussinesq approximations, the governing equations become

$$u = \frac{\partial\psi}{\partial y}, \quad v = -\frac{\partial\psi}{\partial x} \tag{4}$$

$$\frac{\rho_f}{\varepsilon^2}\left(u\frac{\partial u}{\partial x} + v\frac{\partial u}{\partial y}\right) = \rho_f g\beta_f(T - T_\infty) - \frac{\mu_f u}{K} - \rho_f C u^2 + \frac{\mu_f}{\varepsilon}\frac{\partial^2 u}{\partial y^2} \tag{5}$$

$$u\frac{\partial T}{\partial x} + v\frac{\partial T}{\partial y} = \alpha_e\frac{\partial^2 T}{\partial y^2}. \tag{6}$$

These are subject to the following boundary conditions:

$$u = v = 0, \quad T = T_w \quad \text{at} \quad y = 0 \tag{7}$$

$$u = 0, \quad T = T_\infty \quad \text{at} \quad y \to \infty. \tag{8}$$

For low-porosity media, the convective term $\rho\mathbf{u}\cdot\nabla\mathbf{u}$ and the viscous term $\mu\nabla^2\mathbf{u}$, which is responsible for the boundary effect, are usually very small and can be neglected [8, 11]; therefore, the appropriate scaling variables are those given by Cheng and Minkowycz [6]. However, for high-porosity media, the boundary

and convective effects may be important, especially at the upstream end of the heated plate. In this case, different scaling variables should be employed. By assuming the boundary and convective terms to have the same order of magnitude, which implies Pr has order of one, as the buoyancy term, it can be shown that

$$u \sim \nu_f Gr_x^{1/2}/x$$

$$\delta_m \sim x\, Gr_x^{-1/4}$$

$$\psi \sim \nu_f Gr_x^{1/4}$$

where $\nu_f = \mu_f/\rho_f$ is the kinematic viscosity of the fluid, δ_m is the momentum boundary-layer thickness and $Gr_x = g\beta_f \Delta T x^3/\nu_f^2$ is the Grashof number. The scale for the thermal boundary-layer thickness δ_t can be found from the energy equation by balancing the convection and the conduction terms,

$$\delta_t \sim x\, Gr_x^{-1/4}\, Pr^{-1/2}$$

where $Pr = \nu_f/\alpha_e$ is the Prandtl number.

The scaling variables shown above suggest the following nondimensional variables

$$\zeta = \frac{x}{L}, \quad \eta = \frac{y}{x}\left(\frac{Gr_x}{4}\right)^{1/4} \tag{9}$$

$$f = \frac{\psi}{4\nu_f\left(\frac{Gr_x}{4}\right)^{1/4}}, \quad \theta = \frac{T-T_\infty}{T_w-T_\infty} \tag{10}$$

where L is the characteristic length of the heated plate.

In terms of these new variables, the velocity components are given by

$$u = \frac{4\nu_f}{L}\left(\frac{Gr_L}{4}\right)^{1/2}\zeta^{1/2} f_\eta \tag{11}$$

$$v = -\frac{\nu_f}{L}\left(\frac{Gr_L}{4}\right)^{1/4}\zeta^{-1/4}(3f + 4\zeta f_\zeta - \eta f_\eta) \tag{12}$$

and the governing equations (4)–(6) are transformed into

$$-\frac{f_{\eta\eta\eta}}{\varepsilon} + \frac{2f_\eta^2 - 3ff_{\eta\eta}}{\varepsilon^2} + 4\zeta\left(\frac{f_\eta f_{\zeta\eta} - f_\zeta f_{\eta\eta}}{\varepsilon^2} + \zeta^{-1/2}\Phi f_\eta + \Gamma f_\eta^2\right) = \theta \tag{13}$$

$$\theta_{\eta\eta} + 3\,Pr\, f\theta_\eta = 4\,Pr\,\zeta(f_\eta\theta_\zeta - f_\zeta\theta_\eta). \tag{14}$$

The parameters Φ and Γ in equation (13), which characterize respectively the Darcy resistance and the inertia resistance by the porous matrix, are defined as

$$\Phi = 1/(2Gr_L^{1/2}Da_L); \quad \Gamma = LC$$

where the Grashof number, Gr_L, and the Darcy number, Da_L, are given by

$$Gr_L = g\beta_f \Delta T L^3/\nu_f^2$$

$$Da_L = K/L^2.$$

The corresponding boundary conditions at any location ζ along the heated plate are given by

$$f(\zeta, 0) = f_\eta(\zeta, 0) = \theta(\zeta, 0) - 1 = 0 \tag{15}$$

$$f_\eta(\zeta, \infty) = \theta(\zeta, \infty) = 0. \tag{16}$$

When these equations are evaluated at the leading edge, $\zeta = 0$, equations (13)–(16) reduce to those for natural convection from a heated vertical plate in clear media, except for the appearance of ε in the momentum equation. This limiting similarity solution provides the starting solution at the leading edge in the present study.

By defining $\xi = 2\zeta^{1/2}/Gr_L^{1/2}\, Da_L$, equations (13) and (14) can be transformed further into

$$-\frac{f_{\eta\eta\eta}}{\varepsilon} + \frac{2f_\eta^2 - 3ff_{\eta\eta}}{\varepsilon^2} + 2\xi\left(\frac{f_\eta f_{\xi\eta} - f_\xi f_{\eta\eta}}{\varepsilon^2} + \frac{f_\eta}{2} + \xi\,\widehat{Gr}\,\frac{f_\eta^2}{2}\right) = \theta \tag{17}$$

$$\theta_{\eta\eta} + 3\,Pr\, f\theta_\eta = 2\,Pr\,\xi(f_\eta\theta_\xi - f_\xi\theta_\eta) \tag{18}$$

where $\widehat{Gr} = g\beta_f \Delta T K^2 C/\nu_f^2$ is the Darcy-modified Grashof number in porous media [5].

If $\widehat{Gr}$ is very small, inertia effects can be neglected. This may be true for low-porosity media, such as packed beds of small particles. However, for high-porosity media, such as foam materials, $\widehat{Gr}$ can be very large and inertia effects are very significant. Table 1 shows the ranges of the parameters used in this study for three different porous media, with water as the working fluid, for a 1-m-long heated plate. The permeabilities of these foam materials (one producer being Energy Research and Generation, Oakland, California) are 10^{-6}, 10^{-7} and 2.24×10^{-7} m^2, respectively. The inertia coefficient of these materials is assumed to be 200 m^{-1}, which is of the right order for high-porosity foam materials [3].

The local heat transfer rate along the surface of the heated plate can be computed from

$$q = -k_e \left.\frac{\partial T}{\partial y}\right|_0. \tag{19}$$

With the aid of equations (9) and (10), equation (19) can be rewritten as

$$q = -\frac{k_e(T_w - T_\infty)}{x}\left(\frac{Gr_x}{4}\right)^{1/4}\frac{\partial\theta}{\partial\eta}. \tag{20}$$

According to the definition of the local Nusselt number, $Nu_x = qx/(k_e\Delta T)$, equation (20) can be rearranged to

Table 1. Values of ξ and $\widehat{Gr}$ for three different porous media with $Pr = 5.4$, $\Gamma = 200$

Gr_L	Da_L	ξ	$\widehat{Gr}$
10^{11}	10^{-6}	0–6.32	20
	10^{-7}	0–63.2	0.2
2×10^{11}	2.24×10^{-7}	0–20	2

give

$$\frac{Nu_x}{(Gr_x/4)^{1/4}} = -\theta_\eta(\xi, 0) \tag{21}$$

3. BOUNDARY AND CONVECTIVE EFFECTS

When the inertia effect is neglected by setting $\widehat{Gr} = 0$, equations (17) and (18) show that the boundary and convective effects are governed by the parameter ξ. When the permeability is very large and/or the region of interest is at the upstream end of the heated plate, ξ is small and it will be shown that boundary and convective effects are very significant. On the contrary, for large values of ξ, these effects are usually negligible. It should be noted that the boundary-layer approximation can not be applied if ξ is too small. From scaling analysis, boundary-layer analysis is valid for $\xi > \xi_c = Gr_L^{-2/3}\, Da_L^{-1}$. For the three cases considered in Table 1, ξ_cs are 0.046, 0.46 and 0.13, respectively.

3.1. *Asymptotic solution for* $\xi \to 0$

For $\xi \to 0$, the following expansions are assumed

$$f = f_0(\eta) + f_1(\eta)\xi + f_2(\eta)\xi^2 + f_3(\eta)\xi^3 + \cdots \tag{22a}$$

$$\theta = \theta_0(\eta) + \theta_1(\eta)\xi + \theta_2(\eta)\xi^2 + \theta_3(\eta)\xi^3 + \cdots. \tag{22b}$$

The differential equations emerging from this substitution are given in Appendix A. These equations were integrated numerically using the fourth-order Runge–Kutta–Gill method [12]. The derivatives for $Pr = 0.72$ and 5.4 are given in Table 2. The results for $\theta_0'(0)$ and $f_0''(0)$ are close to the previously reported results for a clear media [13]. The difference is due to the presence of the porosity in the coefficients of the boundary and convective terms in equation (5). For highly permeable media ($\varepsilon \to 1$), the difference is expected to be small.

From equations (21) and (22b) the local Nusselt number based on the fourth-order solutions can be written as

$$\frac{Nu_x}{(Gr_x/4)^{1/4}} = -\theta_\eta(\xi, 0) = -[\theta_0'(0) + \xi\theta_1'(0) + \xi^2\theta_2'(0) + \xi^3\theta_3'(0)]. \tag{23}$$

Figures 1 and 2 show the variations of the local dimensionless temperature gradient at the wall for $Pr =$ 0.72 and 5.4, respectively. The local dimensionless temperature gradient, $-\theta'(\xi, 0)$, is related to the local Nusselt number as shown in equation (23). As expected the asymptotic solution is valid only when ξ is small. When compared with solutions by other methods (which is shown in the same figures and will be discussed later), the asymptotic solutions appear to be of satisfactory accuracy in the range $\xi < 4$, but diverge rapidly thereafter. When the value of ξ approaches zero, these solutions approach the solutions when no solid matrix is present.

Table 2. Results for asymptotic solutions

	$Pr = 0.72$		$Pr = 5.4$	
i	$\theta_i'(0)$	$f_i''(0)$	$\theta_i'(0)$	$f_i''(0)$
0	−0.497223	0.652999	−0.964415	0.459267
1	0.058707	−0.107340	0.102196	−0.062547
2	−0.004263	0.016798	0.022481	0.017524
3	−0.000256	−0.001451	0.004764	−0.005317

3.2. *Solution for large* ξ

The region adjacent to the wall, where the vertical velocity increases from the zero value at the wall to the maximum value, can be called the viscous sublayer. As ξ increases, this region progressively occupies a smaller portion of the momentum boundary-layer thickness (this will be shown later). For low-porosity media, the value of ξ is usually large. In this case, the thickness of the viscous sublayer which is caused by the no-slip boundary condition becomes very small; therefore, solutions obtained with the boundary and convective effects neglected are usually satisfactory and the mathematics involved is usually much simpler. By choosing the appropriate nondimensional variables, Cheng and Minkowycz [6] obtained a similarity solution for this situation. Their result was given by

$$\frac{Nu_x}{\widehat{Ra}_x^{1/2}} = 0.444$$

where $\widehat{Ra}_x = g\beta\Delta TKx/\nu_f\alpha_e$ is the Darcy-modified Rayleigh number of the porous medium. In terms of the variables of the present study, the above equation can be rewritten as

$$-\theta'(\xi, 0) = \frac{Nu_x}{(Gr_x/4)^{1/4}} = 0.888\left(\frac{Pr}{\xi}\right)^{1/2}$$

which is plotted as the dashed lines in Figs. 1 and 2.

3.3. *Local non-similarity and finite-difference solutions*

The asymptotic solution is valid for small ξ while Cheng and Minkowycz's solution is valid only for large ξ. To obtain a valid solution for a wider range of ξ, the whole of equations (17) and (18) must be solved. In the present study, both local nonsimilarity [14] and finite-difference solutions based on Keller's Box method [15] are obtained. Results from both methods are presented in Fig. 1, while only the local nonsimilarity solution is presented in Fig. 2. Results in Fig. 1 are for $Pr = 0.72$ while those in Fig. 2 are for $Pr = 5.4$. Also shown in Figs. 1 and 2 are the local similarity solutions. The difference between the local similarity and local nonsimilarity solutions is that in the local nonsimilarity approach, all terms in the momentum and energy equations are retained, and terms are deleted only from subsidiary equations. On the contrary, in the local similarity method, terms which involve the derivatives with respect to ξ are deleted from the momentum and

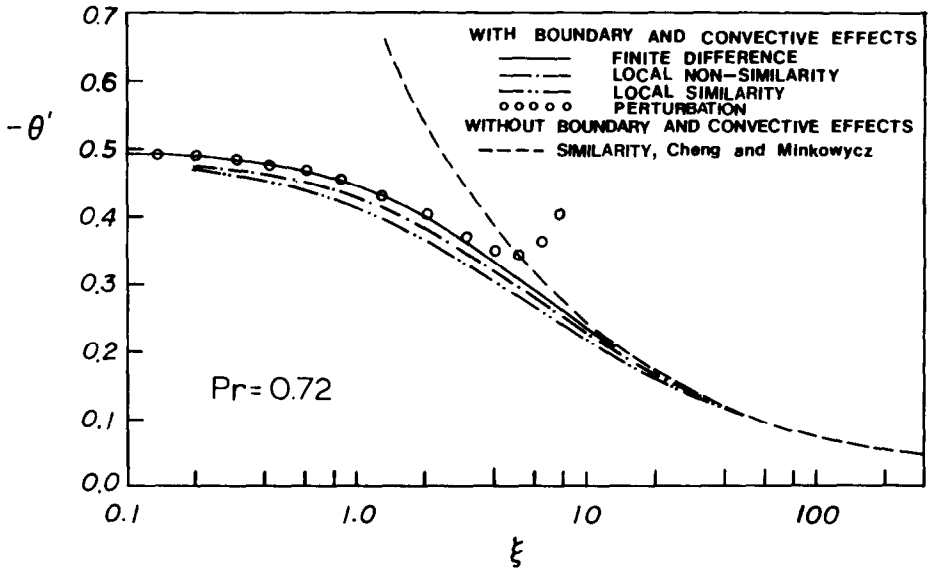

FIG. 1. Variations of local heat transfer results with inertia effects neglected.

energy equations themselves. On this basis, it is expected that the local nonsimilarity method should yield more accurate results than those from local similarity method [14]. When compared with the Box method (Fig. 1) the largest error in the local nonsimilarity method is within 6%, and that for the local similarity method is within 10%.

Both Figs. 1 and 2 show that Cheng and Minkowycz's solution based on Darcy's model is valid only for large values of ξ. When ξ is reduced, the solutions of Cheng and Minkowycz overpredict the heat transfer from the plate due to the neglect of the boundary and convective effects. For the case when $\xi \to 0$, the resistance to the flow is dominated by the boundary and convective effects and the solutions approach those for a clear medium.

Figure 1 shows that the boundary and convective effects can be neglected when ξ is greater than 20 for $Pr = 0.72$. For $Pr = 5.4$, Fig. 2 shows that the limit for ξ is 60. Beyond these limits, Darcy's model can be used to give satisfactory results. Table 1 shows that for high-porosity media, ξ can fall in the range where Darcy's model will incorrectly overpredict the heat transfer. In this case, the boundary and convective effects should be considered.

Figure 3 shows the velocity and temperature

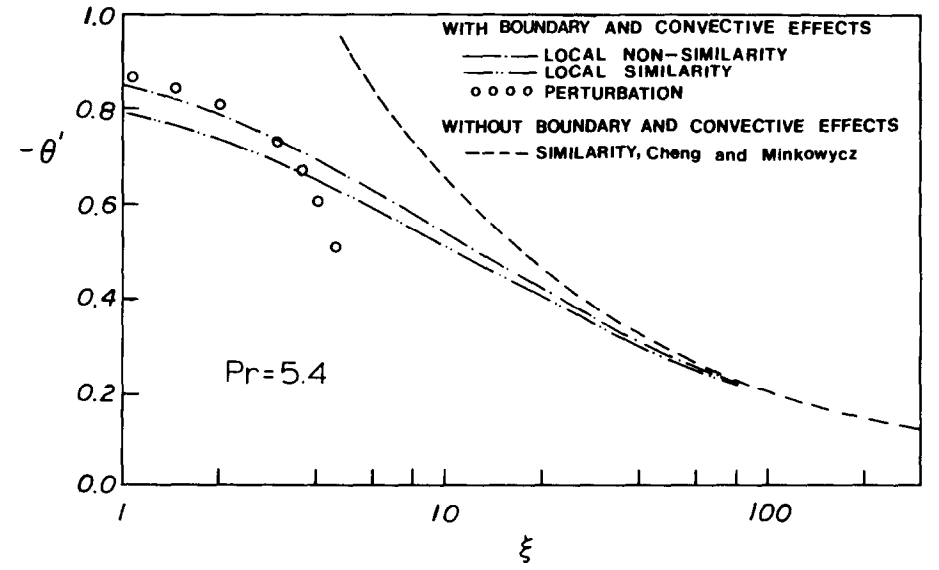

FIG. 2. Variations of local heat transfer results with inertia effects neglected.

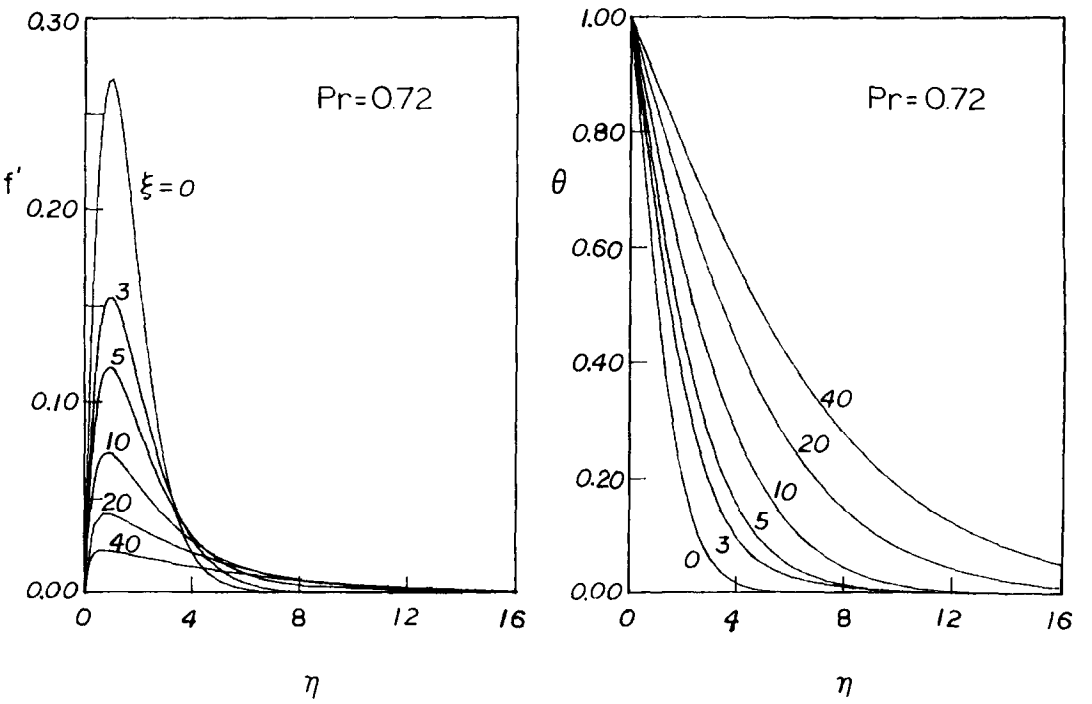

FIG. 3. Velocity and temperature profiles with inertia effects neglected.

distributions for $Pr = 0.72$ at different values of ξ. For small values of ξ, the boundary and convective effects are important, and the profiles look similar to those in a clear medium. When ξ becomes large enough ($\xi = 20$ and 40 in Fig. 3), the Darcy resistance due to the presence of the solid matrix is dominant, and the effect of the no-slip condition is restricted in a viscous sublayer. When the thickness of this viscous sublayer is much smaller than the thickness of the thermal boundary layer, the no-slip condition can be neglected and Darcy's model can be employed.

4. INERTIA EFFECTS

It is well known that when the velocity in porous media is high enough so that the Reynolds number based on the mean pore length scale is greater than one, additional resistance should be incorporated in the analysis. High velocity flow in porous media causes wakes and separation to occur inside the medium, reducing vertical velocities, increasing thermal and hydrodynamic boundary layers and dramatically reducing the heat transfer rate. This inertia effect is usually modeled by a velocity-square term in the momentum equation. When nondimensionalized, the inertia effect is govern by the modified Grashof number $\widehat{Gr}$ as shown in equation (17). From Table 1, it is seen that the modified Grashof number can be quite large for high-porosity media and the inertia effect will then become significant. Considering the inertia effect in addition to the boundary and convective effects, equations (17) and (18) are solved by using the local nonsimilarity method and the results are presented in Figs. 4 and 5.

Figure 4 shows the variation of the local temperature gradient, which is related to the local Nusselt number variation by equation (21), along the vertical heated plate with and without the inertia effect being considered. The ranges of the parameters are those shown in Table 1. The results show that the inertia effect reduces the heat transfer and its effect is more important for higher values of $\widehat{Gr}$. The maximum error of neglecting the inertia effects for $\widehat{Gr} = 0.2, 2$, and 20 are 6, 25 and 60%, respectively. For the same heated plate, the inertia effect increases along the plate because the fluid particles pick up more and more energy along the plate and are accelerated to have higher velocities when they approach the downstream locations.

Figure 5 shows the comparison of the temperature profiles obtained for the case considered in Fig. 4 ($\widehat{Gr} = 2$). Due to the inertia effect, the thermal boundary-layer thickness is increased; the temperature gradient at wall is decreased; and the heat transfer rate is reduced.

From the definition of the modified Grashof number, it is seen that the inertia effect increases with the higher permeability and the lower fluid viscosity. For high-porosity media, small ξ, the boundary and convective effects are important and the inertia effect should also be included; while for low-porosity media, high ξ, in general none of these effects is significant unless the velocity is high enough to induce inertia effect.

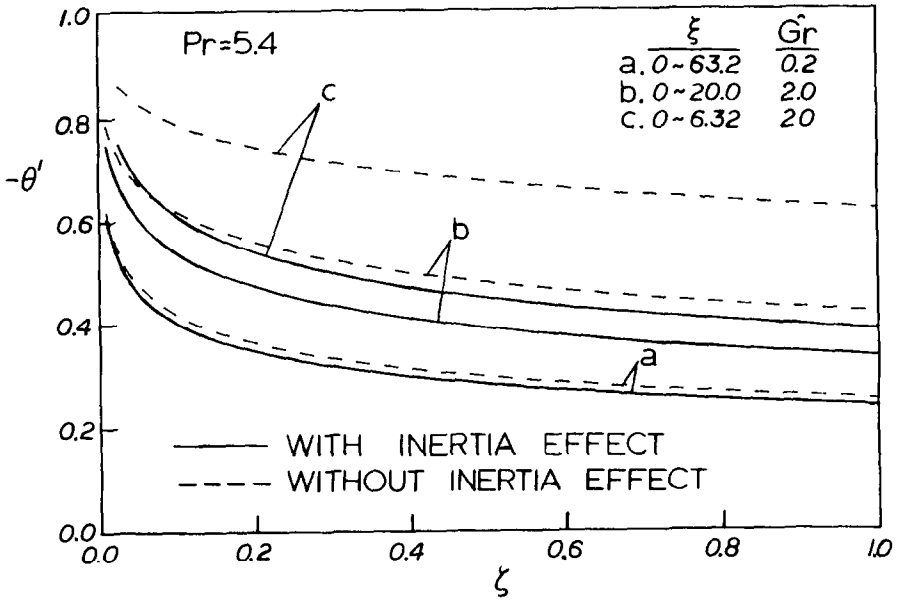

FIG. 4. Variations of local heat transfer results with and without inertia effects.

5. CONCLUSIONS

The purpose of this work is to investigate the significance of the boundary, convective and inertia effects on natural convection from a heated plate embedded in a high-porosity medium. All these effects considered become more important as the permeability of the porous medium increases. A parameter which characterizes the influence of the boundary and convective effects is defined. The numerical results show that when this parameter reaches a certain limit, the conventional solution based on Darcy's model overpredicts the heat transfer. When the inertia effect is considered, the heat transfer is further reduced. This inertia effect is shown to be governed by the modified Grashof number. For porous media with high

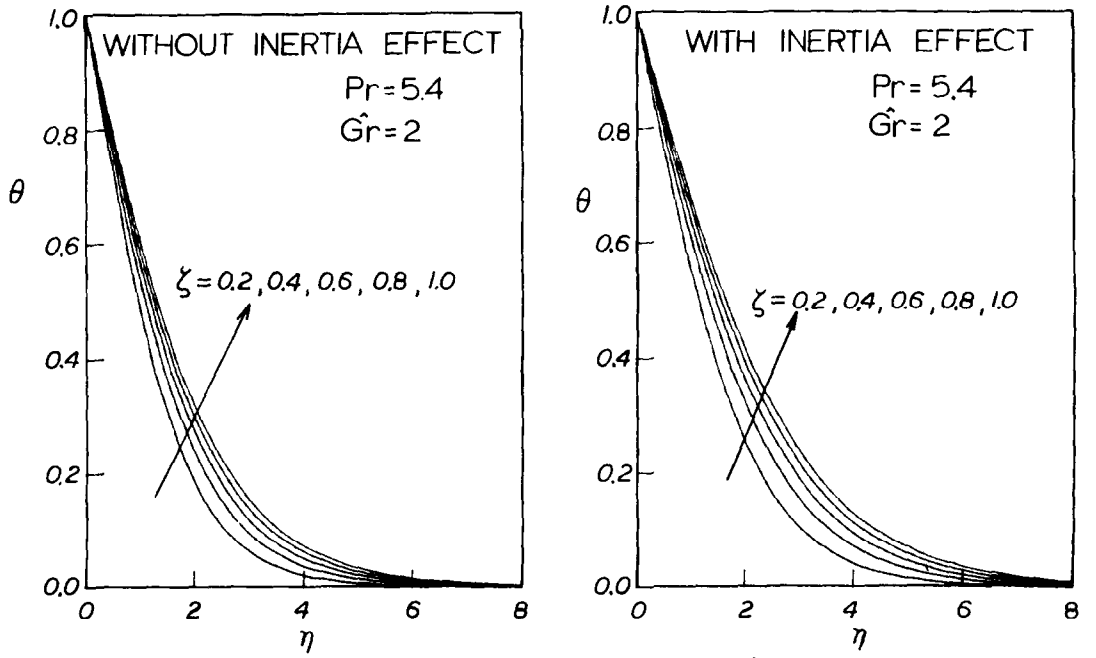

FIG. 5. Comparisons of nondimensional temperature profiles for $\xi = 0$–20, $\widehat{Gr} = 2$ with and without inertia effects.

permeabilities, all the effects considered in this study should be included in the analysis. While for porous media with relatively low permeabilities, all these effects are usually relatively insignificant.

REFERENCES

1. G. S. Beavers and E. M. Sparrow, Non-Darcy flow through fibrous porous media, *J. appl. Mech.* **36,** 711–714 (1969).
2. J. C. Koh, J. L. Dutton, B. A. Benson and A. Fortini, Friction factor for isothermal and nonisothermal flow through porous media, *J. Heat Transfer* **99,** 367–373 (1977).
3. K. Vafai and C. L. Tien, Boundary and inertia effects on flow and heat transfer in porous media, *Int. J. Heat Mass Transfer* **24,** 195–203 (1981).
4. M. Kaviany, Laminar flow through porous media bounded by isothermal parallel plates, *Int. J. Heat Mass Transfer* **28,** 851–859 (1985).
5. P. Cheng, Natural convection in a porous medium: external flows, *Proc. NATO Advanced Study in Natural Convection*, Izmir, Turkey (1985) (in press).
6. P. Cheng and W. J. Minkowycz, Free convection about a vertical flat plate embedded in a porous medium with application to heat transfer from a dike, *J. geophys. Res.* **82,** 2040–2044 (1977).
7. P. Cheng and C. T. Hsu, Higher-order approximations for Darcian free convection flow about a semi-infinite vertical plate, *J. Heat Transfer* **106,** 143–151 (1984).
8. A. Bejan and D. Poulikakos, The non-Darcy regime for vertical boundary layer natural convection in a porous medium, *Int. J. Heat Mass Transfer* **27,** 717–722 (1984).
9. O. A. Plumb and J. C. Huenefeld, Non-Darcy natural convection from heated surfaces in saturated porous media, *Int. J. Heat Mass Transfer* **24,** 765–768 (1981).
10. G. H. Evans and O. A. Plumb, Natural convection from a vertical isothermal surface embedded in a saturated porous medium, ASME Paper No. 78-HT-55 (1978).
11. J. T. Hong, Y. Yamada and C. L. Tien, Effects of non-Darcian and non-uniform porosity on vertical-plate natural convection in porous media, *J. Heat Transfer* (in press).
12. H. J. Romanelli, *Mathematical Methods for Digital Computers* (Edited by A. Ralston and H. Wilf), pp. 110–120. John Wiley, New York (1960).
13. A. J. Ede, Advances in free convection, *Adv. Heat Transfer* **4,** 1–64 (1967).
14. E. M. Sparrow and H. S. Yu, Local non-similarity thermal boundary-layer solutions, *J. Heat Transfer* **4,** 328–334 (1971).
15. H. B. Keller, Numerical methods in boundary-layer theory, *A. Rev. Fluid Mech.* **10,** 417–433 (1978).

APPENDIX

The equations used in the perturbation analysis are obtained by substituting equation (22) into equations (17) and (18) and sorting the like powers of ξ, then one obtains

$$\frac{f_0'''}{\varepsilon}+\frac{3f_0f_0''-2f_0'^2}{\varepsilon^2}=-\theta_0 \tag{A1}$$

$$\frac{f_1'''}{\varepsilon}+\frac{3f_0f_1''+5f_1f_0''-6f_0'f_1'}{\varepsilon^2}-f_0=-\theta_1 \tag{A2}$$

$$\frac{f_2'''}{\varepsilon}+\frac{3f_0f_2''+7f_2f_0''+5f_1f_1''-4f_1''^2-8f_0'f_2'}{\varepsilon^2}-f_1'=-\theta_2 \tag{A3}$$

$$\frac{f_3'''}{\varepsilon}+\frac{3f_0f_3''+7f_2f_1''+5f_1f_2''+9f_3f_0''-10f_2'f_1'-10f_3'f_0'}{\varepsilon^2}$$

$$-f_2'=-\theta_3 \tag{A4}$$

$$Pr^{-1}\theta_0''+3f_0\theta_0'=0 \tag{A5}$$

$$Pr^{-1}\theta_1''+3f_0\theta_1'+5\theta_0'f_1-2\theta_1f_0'=0 \tag{A6}$$

$$Pr^{-1}\theta_2''+7f_2\theta_0'+5f_1\theta_1'+3f_0\theta_0'-2f_1'\theta_1-4f_0'\theta_2=0 \tag{A7}$$

$$Pr^{-1}\theta_3''+9f_3\theta_0'+7f_2\theta_1'+5f_1\theta_2'+3f_0\theta_3'-4f_1'\theta_2-6f_0'\theta_3=0 \tag{A8}$$

where the primes indicate derivatives with respect to η.

The boundary conditions for equations (A1)–(A8) are

$$\eta=0:\quad f_i=f_i'=0,\qquad i=0,1,2,3,\ldots$$

$$\theta_0=1,\ \theta_i=0,\quad i=1,2,3,\ldots$$

$$\eta=\infty:\quad f_i'=\theta_i=0,\qquad i=0,1,2,\ldots.$$

EFFETS NON DARCIENS DANS LA CONVECTION NATURELLE SUR PLAQUE VERTICALE DANS UN MILIEU POREUX A GRANDE POROSITE

Résumé—L'étude analytique des effets non Darciens sur la convection naturelle autour d'une plaque verticale noyée dans un milieu très poreux montre que les effets de frontière et d'inertie ont une influence significative sur les profils de vitesse et sur les flux thermiques à la paroi. Les deux effets sont plus prononcés dans les milieux à forte porosité et ils réduisent le transfert thermique de la paroi chaude. L'effet de frontière devient notable dans la région proche du bord d'attaque de la plaque chaude, tandis que l'effet d'inertie augmente avec la position sur la plaque chaude. Les résultats montrent aussi que lorsque la résistance due à la matrice solide augmente, le profil de vitesse tend vers la forme exponentielle conventionnelle qui résulte d'un glissement de vitesse à la frontière.

NATÜRLICHE KONVEKTION AN EINER SENKRECHTEN PLATTE IN EINEM HOCHPORÖSEN MEDIUM (NON-DARCY-EFFEKTE)

Zusammenfassung—Die vorliegende analytische Untersuchung von Effekten, die nicht dem Darcy'schen Gesetz folgen, zeigt, daß bei der natürlichen Konvektion an einer senkrechten Platte in einem hochporösen Medium Wand- und Trägheitseffekte einen bedeutenden Einfluß auf Geschwindigkeitsprofile und Wärmeübergang haben. Beide Effekte sind in Medien von hoher Porosität stärker ausgeprägt und vermindern den Wärmeübergang an der beheizten Platte. Der Wand-Einfluß ist im Bereich der Plattenunterkante von größerer Bedeutung, während sich die Trägheitseffekte weiter oben stärker auswirken. Die Ergebnisse zeigen auch, daß mit zunehmendem Durchflußwiderstand der festen Phase das Geschwindigkeitsprofil immer mehr die konventionelle exponentielle Form annimmt, was auf einen Schlupf an der Wand zurückzuführen ist.

ВЛИЯНИЕ ЭФФЕКТОВ, НЕ ПОДЧИНЯЮЩИХСЯ ЗАКОНУ ДАРСИ, НА ЕСТЕСТВЕННУЮ КОНВЕКЦИЮ ОТ ВЕРТИКАЛЬНОЙ ПЛАСТИНЫ В ПОРИСТЫХ СРЕДАХ С ВЫСОКОЙ СТЕПЕНЬЮ ПОРИСТОСТИ

Аннотация—Анализ влияния на естественную конвекцию от вертикальной пластины, погруженной в высокопористую среду, эффектов, не подчиняющихся закону Дарси, показывает, что граничные и инерционные эффекты оказывают существенное влияние на профили скорости и коэффициент теплоотдачи. И те и другие эффекты больше проявляются в высокопористых средах и уменьшают теплоотдачу от нагретой пластины. Граничный эффект становится более заметным в зоне, прилегающей к передней кромке нагреваемой пластины, в то время как инерционный эффект возрастает в области, расположенной на пластине вниз по потоку. Результаты также показывают, что как только возрастает сопротивление, вызванное твердой матрицей, профиль скорости приобретает обычную экспоненциальную форму, которая является результатом проскальзывания на границе.